Computers & Industrial Engineering 185 (2023) 109679

Contents lists available at ScienceDirect

Computers & Industrial Engineering

journal homepage: www.elsevier.com/locate/caie

Similarity searching for fault diagnosis of defect patterns in wafer bin maps ☆

Rui Wang [a], Songhao Wang [b,*]

[a] School of Mechanical Engineering and Automation, Harbin Institute of Technology, Shenzhen, China
[b] School of Business, Southern University of Science and Technology, Shenzhen, China

ARTICLE INFO

Keywords:
Similarity searching
Wafer bin map
Defect diagnosis
Yield enhancement
Semiconductor manufacturing

ABSTRACT

Due to the growing complexity of processes in semiconductor manufacturing, high volumes of data are automatically generated, resulting in a greater challenge for fault detection and yield improvement. Wafer bin maps (WBMs), which represent the spatial distribution of defective dies on the wafer, may contain specific defect patterns that offer useful insight into the underlying causes of anomalies in the processes. Hence, the identification of these defect patterns helps the early detection and diagnosis of the faults. Nowadays, rare and mixed-type defects are more frequently observed, which increases the difficulty for the recognition of defect patterns. In this study, we propose a similarity searching approach for the identification of defect patterns and their potential causes. The comparison of similar patterns provides valuable information to trace the problems in the process history which may narrow the scope of troubleshooting. In particular, the tensor voting algorithm is applied to highlight the structural information in the patterns, and then the weighted best-buddies similarity (WBBS) is proposed to measure the degree of similarity. Experimental results verify the effectiveness of the proposed method in the context of both single and mixed-type defect patterns.

1. Introduction

The semiconductor manufacturing is a sophisticated and lengthy process with hundreds of steps, during which errors are inevitable. Yield improvement has become a critical concern to guarantee high-quality products and low costs at the same time (Dou, He, & Hsu, 2018). Nowadays, technique advances allow the collection of data that are seen to be of complex structure and increasingly high volume (Li, Du, Huang, Zhao, & Deng, 2019; Li, Du, Wang, Lv, & Deng, 2022). With the help of the acquired data, it is possible to extract valuable information to monitor the system quality (Zhang, Yan, Lee, & Shi, 2018a, 2018b), detect anomalies (Zhu, Huang, Shen, & Shen, 2022), suggest solutions (Qin et al., 2020) and ultimately improve process yield (Huang, Du, Li, & Wu, 2017). The wafer bin map (WBM), in particular, is a two-dimensional graphic depiction of a wafer where each pixel indicates the functionality of each die. It is produced following the circuit probe (CP) yield test, which evaluates the electrical functionality of each die on the wafer following wafer fabrication. The CP test is an important yield indicator that helps with low yield troubleshooting, failure monitoring and diagnosis, and performance enhancement. The quality of the CP test is illustrated with the WBM, which typically contains both random defects that are randomly distributed, as well as systematic defects that exhibit spatial correlations (Liao, Hsieh, Huang, & Chien, 2014). The WBM attracts much attention as the systematic defects may form specific patterns that are caused by assignable failures in the process. The analysis of the patterns allows engineers to trace the problem back in history for fault diagnosis and root cause detection, which is beneficial for yield enhancement and cost reduction. In practice, the identification and comparison of the patterns are mostly conducted by engineers through visual inspection, and are heavily dependent on domain knowledge and expertise. Such human-eye based judgement may be subjective, time-consuming and lack of consistency (Kyeong & Kim, 2018).

To overcome the challenge of high inspection costs and yield loss associated with defective dies, many studies have been conducted for WBM analysis, and they can be divided into two categories: unsupervised and supervised approaches. Unsupervised learning is able to group the samples into clusters without pre-determined labels. For example, Hsu and Chien (2007) proposed a hybrid data mining approach that integrates spatial statistics and adaptive resonance theory (ART) neural networks to extract patterns from WBMs. Lee, Yu, and Park (2001) clustered the chip locations having similar defect features through self-organizing map (SOM) neural networks. Hwang and Kim

☆ This work was supported in part by the National Natural Science Foundation (NNSF) of China under Grant 72101065 and Grant 72101106, in part by the Guangdong Basic and Applied Basic Research Foundation under Grant 2021A1515110336, and in part by the Shenzhen Science and Technology Program under Grant RCBS20221008093124063 and Grant RCBS20210609103119020.

* Corresponding author.
E-mail addresses: r.wang@hit.edu.cn (R. Wang), wangsh2021@sustech.edu.cn (S. Wang).

https://doi.org/10.1016/j.cie.2023.109679
Received 24 June 2023; Received in revised form 14 September 2023; Accepted 10 October 2023
Available online 12 October 2023

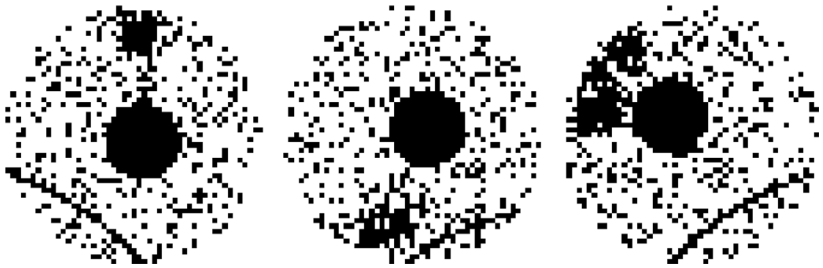

Fig. 1. Examples of WBMs with mixed-type patterns.

(2020) performed one-step clustering with a Gaussian mixture model applied to a variational autoencoder (VAE) framework. Supervised learning is able to recognize existing patterns, but cannot identify newly-emerged defect patterns. In recent years, machine learning methods were applied for WBM classification, including support vector machine (SVM) (Wu, Jang, & Chen, 2014), decision tree (Piao, Jin, Lee, & Byun, 2018) and linear discriminant analysis (LDA) (Yu & Lu, 2015). Deep learning-based approaches have received an increased amount of interest recently because of their excellent capability in image processing and applicability in various fields. In Adly et al. (2015), General regression neural network (GRNN) was proposed for the accurate and efficient identification of defect patterns in WBMs. The most popular solution is the convolutional neural networks (CNNs), which is specifically developed for image data, examples of these models are seen in Hsu and Chien (2022), Kang and Kang (2021), Nakazawa and Kulkarni (2018).

In modern wafer manufacturing systems, mixed-type defect patterns which contains two or more single pattern in the same WBM, are frequently observed because of the increasing circuits density and wafer design complexity. For mixed-type patterns, several manufacturing problems can be found, with each defect pattern having a related root cause (Yuan & Kuo, 2008). Fig. 1 illustrates examples of the same mixed-type defect pattern consisting of "Scratch", "Center" and "Loc" patterns. "Scratch" patterns are generated by machine handling problems, "Center" patterns are caused by uniformity variations in the chemical mechanical process (CMP), while "Loc" patterns are generated by non-uniformity or uneven cleaning (Kim, Lee, & Kim, 2018). In Fig. 1, both systematic defects that forms certain patterns, and random defects that are seen as noise to the patterns, are seen in the same WBM. In addition, the combination of sizes and placements of various single patterns may also vary significantly, making it more challenging to recognize mixed-type patterns. For the classification of mixed-type defect patterns in WBMs, a few deep learning based models have been proposed. Kyeong and Kim (2018) used a mixture of each pattern's distinct CNN-based classification model to recognize mixed-type defect patterns. Wang, Xu, Yang, Zhang, and Li (2020) introduced a deformable convolutional network to extract high-quality features for mixed-type pattern recognition. Shin, Kahng, and Kim (2022) suggested utilizing samples with single type patterns to train CNNs in WBMs with a Mixup-based strategy for the classification of mixed-type patterns.

Existing approaches provide solutions for automatic recognition of defect patterns in both single and mixed-type scenarios. However, these classification based methods may have limitations that they cannot distinguish the similarity of different WBMs regarding a query one, resulting in the misdiagnosis when tracking in the history, if the patterns are not significantly similar (Liao, Hsieh, Huang, & Chien, 2013). Furthermore, existing methods cannot give satisfactory results when recognizing a newly or rarely observed pattern. In order to improve the efficiency and effectiveness for the tracking of root causes, similarity measures between two WBMs are considered for the WBM analysis. Similarity searching makes it possible to identify root causes by tracing the process history using similarity as a criterion, which limits the scope of troubleshooting and lowers the risk of misdiagnosis (Hsu, Chen, & Chien, 2020). However, the determination of similarity measure is challenging because the similarity defined by human experts is intrinsically subjective. In addition, the patterns in the each class may also vary in noise level, pattern location and wafer rotation, etc. These factors need to be carefully considered in the design of the similarity measure.

Few studies have focused on WBM similarity searching. The majority of the studies that examines similarity measurement of WBMs involve the training of supervised models, which may not guarantee performance when labels are unknown, as the features for similarity ranking are learned using labeled data (Liao et al., 2013; Nakazawa & Kulkarni, 2018). To address this issue, Wu et al. (2014) developed a set of novel rotation- and scale-invariant features without pre-determined pattern labels, and similar WBMs are found based on the Euclidean distance of the extracted features. Hsu et al. (2020) proposed a similarity ranking method without pattern labels by calculating the Hausdorff distances of enhanced feature maps generated by a mountain clustering algorithm. Lee, Moon, and Oh (2021) first used nonparametric Bayesian clustering to find local clusters and then employed hierarchical clustering to obtain the global clusters with a weight vector, which are subsequently applied to measure and rank similarity. However, existing methods mainly deal with single type defect patterns, which lacks the adaptability for mixed-type patterns that appears to be complex, which includes patterns varying in different sizes and locations with interactions. For mixed-type patterns, however, the root causes corresponding to the isolated single patterns are independent. That is, a WBM may contain multiple patterns, with only one pattern having the same root cause with the query one. In order to provide comparable scores with the same pattern contained in different WBMs, the similarity measure must be properly created. It must also take into account the exact similarity when the number of faulty points actually varies.

This study proposes a method for WBM similarity searching to support decision making of engineers for root cause detection and yield enhancement. We put forward a similarity measurement model and develop the related similarity indices for the ranking and query of similar patterns. The proposed method is based on the preliminary work in Wang and Wang (2022). Tensor voting (Mordohai & Medioni, 2010), a perceptual grouping technique, is initially used to transform the WBMs in order to retrieve structural information. In tensor voting, information about the local structural features is propagated across the neighborhood. As a result, points that belong to the same structure will give coherent structural information, which can then be used to find salient structures (Du, Yan, Chang, & Shi, 2022). We are motivated to use the tensor voting algorithm for feature transformation because of its inherent robustness to noise and capacity for handling complex patterns. Then, a weighted best-buddies similarity (WBBS) algorithm is proposed to measure the similarity of mixed-type WBMs. The method is validated with experiments using simulated patterns generated by the method described in Kyeong and Kim (2018). The main contributions of this study are summarized as follows:

- The proposed method enables similarity searching in the context of both single and mixed-type patterns.
- The proposed method can be used for WBM identification, while variations in shapes are considered regarding the same type of defect patterns.

- The proposed method is able to search for similar patterns without model training and the collection of large amount of data.

The remainder of this paper is organized as follows. In Section 2, we describe the proposed WBM similarity searching method. The experimental results are analyzed in Section 3. Section 4 presents discussions and possible improvements of the proposed method. Section 5 concludes this paper and highlights future research directions.

2. Methodology

In this section, we propose a novel similarity searching approach in WBMs, which can be applied when the defect patterns appear to have mixed types with noise. To obtain structural saliency of the defects, the tensor voting algorithm is first applied to original WBMs. Based on the results of tensor voting, the noisy defects are removed to emphasize the pattern structures and improve the data quality. Then, a similarity measure is proposed to properly evaluate the similarity between WBMs with robustness to background, occlusions and complex deformations. The detailed description of the proposed method is presented in the following subsections.

2.1. Tensor voting based feature transformation

The raw WBM is a binary valued image that contains only the functional information of each die. Therefore, it is hard to infer specific patterns directly based on the original WBM data. Conventionally, in semiconductor industry, the mountain function (Yager & Filev, 1994) is used to compute the density of the surrounding pixels around a given point on an image in order to obtain the spatial distribution of the patterns (Liao et al., 2014). The mountain clustering method gives the clustering features of the defective dies, but it cannot represent different structures that make up of the WBM such as curves and regions. The tensor voting is a perceptual grouping method which aims to extract salient features from clouds of points without prior knowledge (Medioni, Tang, & Lee, 2000). It has shown great power to infer structural information based on good continuation and proximity under the existence of gaps and noise. Specifically, in 2-D, the tensor voting is able to distinguish curves, junctions and regions from corrupted images, which provides a chance to amplify the pattern related features in the WBMs. In the following, we present a brief introduction to a closed-form solution to tensor voting algorithm (Wu, Yeung, Jia, Tang, & Medioni, 2011).

The tensor voting proposes that the arrangement of the surrounds, rather than the individual points, determines the structural saliency. In particular, a tensor vote is cast from the voter to the vote receiver subject to proximity and continuity requirements. In Fig. 2, two points $\mathbf{x}_i \in \mathbb{R}^d$ and $\mathbf{x}_j \in \mathbb{R}^d$ are connected by some smooth structure, the unit normal $\mathbf{n}_j$ is the voting tensor, $\mathbf{r}_{ij}$ is a unit vector at $\mathbf{x}_j$ pointing to $\mathbf{x}_i$, and $\mathbf{v}_i$ is the normal vote received at $\mathbf{x}_i$ derived by the osculating arc between the two points.

First, the special case when $\mathbf{n}_j$ is known is considered. The structure-aware tensor $\mathbf{K}_i \in \mathbb{R}^d \times \mathbb{R}^d$ at $\mathbf{x}_i$ can be calculated in the form of a second-order symmetric tensor, which is equivalent to a $d \times d$ matrix and can be visualized as ellipsoid. $\mathbf{K}_i$ is defined as $\mathbf{v}_i\mathbf{v}_i^T$ multiplied by $\eta(\mathbf{x}_i, \mathbf{x}_j, \mathbf{n}_j)$, where

$$\eta(\mathbf{x}_i, \mathbf{x}_j, \mathbf{n}_j) = c_{ij}(1 - (\mathbf{r}_{ij}^T\mathbf{n}_j)^2), \tag{1}$$

$$c_{ij} = \exp(-\frac{\left\|\mathbf{x}_i - \mathbf{x}_j\right\|^2}{\sigma_d}). \tag{2}$$

In (1) and (2), $1-(\mathbf{r}_{ij}^T\mathbf{n}_j)^2$ is a square-sine function which panelizes the curvature, σ_d is the scale parameter which denotes the size of neighborhood considered for voting. The definition of $\eta(\mathbf{x}_i, \mathbf{x}_j, \mathbf{n}_j)$ implies that smooth continuation and closeness are preferred in the computation of the structure-aware tensor vote.

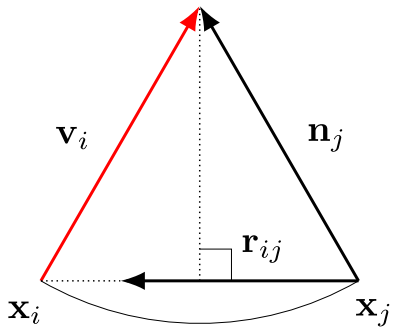

Fig. 2. Second order vote cast by a stick tensor at O to P.

Then, the general case is considered where the normal $\mathbf{n}_j$ at $\mathbf{x}_j$ is unknown. Let $\mathbf{K}_j$ at $\mathbf{x}_j$ be any second-order symmetric tensor, which is typically initialized as an identity matrix. Then the set of all possible unit normals $\{\mathbf{n}_{\theta j}\}$ associated with the corresponding length $\{\tau_{\theta j}\}$ at all possible directions θ of $\mathbf{K}_j$ are considered for vote computation. The tensor vote $\mathbf{S}_{ij}$ obtained at $\mathbf{x}_i$ induced by $\mathbf{K}_j$ located at $\mathbf{x}_j$ is:

$$\mathbf{S}_{ij} = \int_{\mathbf{N}_{\theta j} \in \nu} \mathbf{v}_\theta(\mathbf{x}_i, \mathbf{x}_j)(\mathbf{x}_i, \mathbf{x}_j)^T \eta(\mathbf{x}_i, \mathbf{x}_j, \mathbf{n}_{\theta j}) d\mathbf{N}_{\theta j}, \tag{3}$$

where

$$\mathbf{N}_{\theta j} = \mathbf{n}_{\theta j}\mathbf{n}_{\theta j}^T, \tag{4}$$

and ν is the space of all possible $\mathbf{N}_{\theta j}$. Based on the osculating arc connection shown in Fig. 2, we have

$$\mathbf{v}_\theta(\mathbf{x}_i, \mathbf{x}_j) = (\mathbf{n}_{\theta j} - 2\mathbf{r}_{ij}(\mathbf{r}_{ij}^T\mathbf{n}_{\theta j}))\tau_{\theta j}. \tag{5}$$

The closed-form solution of the structure-aware tensor $\mathbf{K}_i$ at each site $\mathbf{x}_i$ is the accumulation of all the votes cast from the neighborhood, which is given in Wu et al. (2011) as follows:

$$\mathbf{K}_i = \sum_j \mathbf{S}_{ij}, \tag{6}$$

$$\mathbf{S}_{ij} = c_{ij}\mathbf{R}_{ij}\mathbf{K}_j(\mathbf{I} - \frac{1}{2}\mathbf{r}_{ij}\mathbf{r}_{ij}^T)\mathbf{R}_{ij}^T, \tag{7}$$

with

$$\mathbf{R}_{ij} = \mathbf{I} - 2\mathbf{r}_{ij}\mathbf{r}_{ij}^T. \tag{8}$$

In the WBM, a second-order symmetric tensor $\mathbf{K}_i$ is equivalent to a 2×2 matrix, which can be decomposed as:

$$\mathbf{K}_i = \lambda_1\vec{e}_1\vec{e}_1^T + \lambda_2\vec{e}_2\vec{e}_2^T, \tag{9}$$

where $\vec{e}_1$ and $\vec{e}_2$ are the eigenvectors of $\mathbf{K}_i$ whose corresponding eigenvalues are λ_1 and λ_2 ($\lambda_1 \geq \lambda_2$). The tensor defined in (9) can be further decomposed into the stick and ball components:

$$\mathbf{K}_i = \lambda_s\mathbf{T}_s + \lambda_b\mathbf{T}_b, \tag{10}$$

where $\mathbf{T}_s = \vec{e}_1\vec{e}_1^T$ is a stick tensor and $\mathbf{T}_b = \vec{e}_1\vec{e}_1^T + \vec{e}_2\vec{e}_2^T$ is a ball tensor. $\lambda_s = \lambda_1 - \lambda_2$ is called stick saliency, which is a measure of the confidence of the encoded direction. $\lambda_b = \lambda_2$ denotes ball saliency, which measures the degree that the point's underlying structure is unoriented. The combination of stick and ball saliency gives hints on the structure that the point belongs to. When $\lambda_s \approx 0$ and $\lambda_b > 0$, the structure indicates no orientation preference, so the point may lies in a region or junctions of curves. Similarly, when $\lambda_s > 0$ and $\lambda_b \approx 0$, the tensor is nearly a stick tensor that shows a direction with the strength λ_s, indicating a curvature structure.

Given that defect patterns in the WBMs mostly consist of curves (such as "Edge" and "Scratch") and regions (such as "Center" and "Donut") structures, the application of tensor voting for feature transformation is advantageous for the analysis of these defect patterns. The

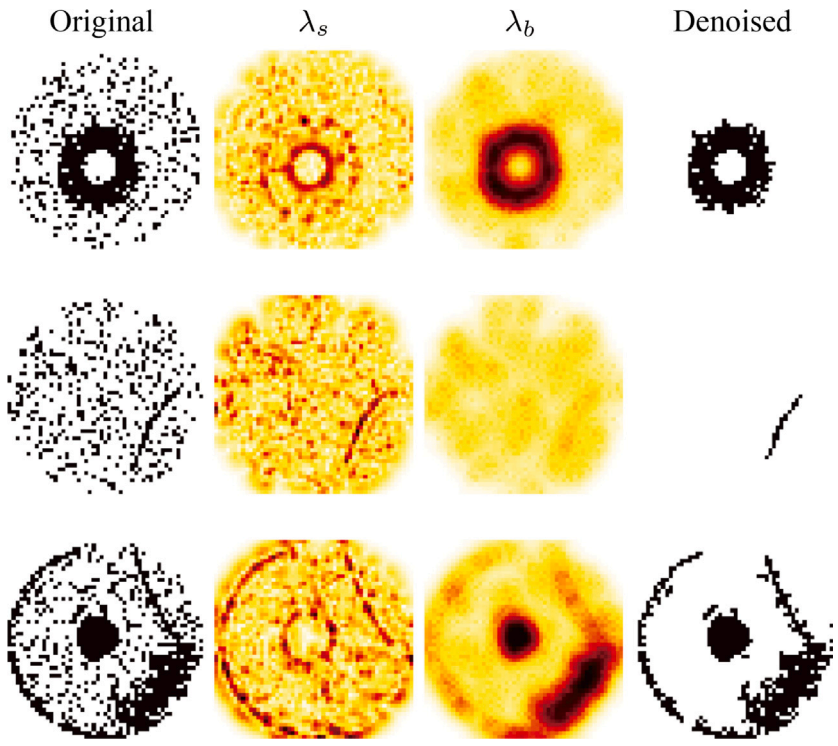

Fig. 3. Results of tensor voting based feature transformation.

results of tensor voting is also ideal for the removal of isolated defective points, which provide lower saliency values on the map of both λ_s and λ_b due to the inconsistent appearance that does not belong to any specific structure. The noisy points are removed with thresholding method when both $\lambda_s < t * \max(\lambda_s)$ and $\lambda_b < t * \max(\lambda_b)$, where t denotes the percentage of saliency value that are regarded as noise.

Fig. 3 shows examples of the structural and ball saliency computed by tensor voting, as well as the WBMs after noise removal. The first column in Fig. 3 shows the raw WBMs, the second and third columns illustrate the stick and ball saliency, respectively. In color structured points that are a part of a pattern, the stick and ball saliency is darker, therefore the isolated points can be eliminated. The last column is the denoised WBMs based the results of tensor voting. The WBM in the first row contains a "Donut" pattern in the middle of the wafer. The stick saliency appears darker only at the region edge, while the ball saliency highlights concentrated area. The "Scratch" pattern has higher value in the map of stick saliency in the second row. The third row in Fig. 3 is a mixture of patterns, the appearance of the stick and ball saliency map are consistent with that in the single-patterned WBM, demonstrating the capacity of tensor voting to extract structural information that can be used for similarity measurement.

2.2. Similarity measure

Based on the information obtained from tensor voting, we attempt to compare the patterns in the WBMs after noise removal. A template matching approach called the best-buddies similarity (BBS) (Oron, Dekel, Xue, Freeman, & Avidan, 2017) is applied to evaluate the similarity between two WBMs. Both the structural saliency and location information of the denoised WBMs are considered for the computation of the similarity measure. BBS is inherently robust to outliers, because it only counts the pair of points that are mutual nearest neighbors, which is also known as best-buddies pairs (BBPs). In addition, BBS has the property that the maximum BBS value reaches only when the two groups of points to be compared are drawn from the same distribution, and the result decreases sharply as the distribution diverge.

In the context of WBM similarity searching, BBS is defined to measure the similarity between the selected template and the WBMs to compare in the history. The two sets of points are denoted as $P = \{p_i\}_{i=1}^{N}$ and $Q = \{p_i\}_{i=1}^{M}$, $p_i, q_j \in \mathbb{R}_d$, respectively. A pair of points is considered a BBP, if for a pair of points $\{p_i \in P, q_j \in Q\}$, p_i is the nearest neighbor of q_j in Q, and q_j is the nearest neighbor of p_i in P. Then BBP can be formulated as an indicator function,

$$bb(p_i, q_j, P, Q) = \begin{cases} 1, & NN(p_i, Q) = q_j \wedge NN(q_j, P) = p_i \\ 0, & \text{otherwise} \end{cases} \tag{11}$$

where $NN(p_i, Q) = \arg\min_{q_j \in Q} d(p_i, q_j)$ is the nearest point of q_j in Q, and $d(p_i, q_j)$ is the distance between p_i and q_j. The function takes value 1 if a BBP is satisfied.

Initially, BBS is defined to compare two images of the same size. However, the number of defective points varies in different WBMs, so here a weight is included to compare these patterns. The weight can be divided into two parts: the weight w_p for the number of points in the two sets, and the weight w_v for the variations in the number of points to be compared in the history. The distance of the weighted BBS between the point sets P and Q is given by:

$$WBBS(P, Q) = w_p w_v \cdot \sum_{i=1}^{N} \sum_{j=1}^{M} bb(p_i, q_j, P, Q). \tag{12}$$

Basically, the number of BBPs should be smaller than the minimum number of the points in P and Q, and the weight w_p can be represented as follows:

$$w_p = \frac{1}{\min(N, M)}, \tag{13}$$

so that the similarity satisfies the commutative property $WBBS(P, Q) = WBBS(Q, P)$. As BBS only considers the number of pairs that have the mutually nearest distance, the BBS will give similar results for both single and mixed-type patterns if they contain the query pattern. To panelize the variation in the number of defective dies on the WBMs, the weight is specially designed as:

$$w_v = \exp(-\frac{\alpha |N - M|}{l}), \tag{14}$$

Predicted Class \ Actual Class	Contain pattern *c*	Do not contain pattern *c*
Contain pattern *c*	True Positive (TP)	False Positive (FP)
Do not contain pattern *c*	False Negative (FN)	True Negative (TN)

Fig. 4. Confusion matrix of similarity searching in mixed-type patterns.

where l is the total number of dies on the WBM which is fixed for the same type of the wafer product, and α is the scale parameter that controls the degree of similarity difference for single or mixed-type patterns. The greater value of $WBBS$ indicates higher similarity between template P and target Q.

Both the structural saliency and the location of defects should be taken into account for the similarity measurement of WBMs. Curves and areas can be separated by structural saliency, while the specific patterns of the defect clusters can be determined by the locations. For example, "Center" and "Loc" patterns show similar results in the ball saliency map, but the "Center" pattern appear much closer to the wafer center. Then the distance measure is defined as a tradeoff between structural and location information:

$$d(p_i, q_j) = \left\| p_i^{(S)} - q_j^{(S)} \right\|_2^2 + \mu \left\| p_i^{(L)} - q_j^{(L)} \right\|_2^2, \tag{15}$$

where superscripts S and L denote the descriptor of structural saliency and location, respectively, and μ is a parameter that controls the weight of the strength between structure saliency and the location information. The structural descriptor is the stick and ball saliency (λ_s, λ_b). The location information is described by polar coordinates ρ, defined as

$$\rho = \sqrt{a^2 + b^2}, \tag{16}$$

where ρ is the distance from the origin, when the point is located at (a, b) in Cartesian coordinates. Both of the descriptors are normalized to the range $[0, 1]$.

2.3. Model evaluation

To evaluate the similarity between two WBMs, we examine the problem of binary classification, i.e., if the WBM contains the query pattern c, for the identification of mixed-type patterns. If the similarity measure is higher than a certain threshold, the WBM is predicted to include the query pattern c.

The combination of actual and predicted classes has four results: true positive (TP), false positive (FP), true negative (TN) and false negative (FN), as shown in Fig. 4. True positive rate (TPR) and false positive rate (FPR) are defined as:

$$\mathrm{TPR} = \frac{\mathrm{TP}}{\mathrm{TP} + \mathrm{FN}}, \tag{17}$$

$$\mathrm{FPR} = \frac{\mathrm{FP}}{\mathrm{FP} + \mathrm{TN}}. \tag{18}$$

The receiver operating characteristic (ROC) curve, which plots TPR vs. FPR at different classification thresholds, is used to evaluate the performance of the proposed method.

The precision–recall (PR) curve is additionally applied to evaluate the detection performance on imbalanced data, as the ROC curves are overly optimistic when the amount of positive examples is far less than negative ones (Saito & Rehmsmeier, 2015). Specially, the pattern "Random" and "Near-full" are single-type patterns and cannot mix with others, showing classes imbalance in the task of binary classification. The precision (Pc) and Recall (Rc) defined at every threshold are:

$$\mathrm{Pc} = \frac{\mathrm{TP}}{\mathrm{TP} + \mathrm{FP}}, \tag{19}$$

$$\mathrm{Rc} = \frac{\mathrm{TP}}{\mathrm{TP} + \mathrm{FN}}. \tag{20}$$

It should be noted that the definition of TPR and Rc is the same, where TPR=Rc in the two curves. For ROC, the Area under the curve (AUC) is used to measure the classification performance. The average precision (AP), which computes the area under the PR curve, is also applied as a numeric metric. Higher values of both indices indicate the effectiveness of the method.

3. Experiments

We used the dataset "MixedWM38" provided in Wang et al. (2020) to evaluate the performance of the proposed method. The dataset contains both real-world defect patterns, as well as simulated ones to guarantee class balance. Frequently occurred mixed-type patterns are collected, which are defined as combinations of basic defect patterns. When similarity searching in mixed-type patterns, the pattern "Edge-ring" and "Edge-Loc" can be regarded as the same pattern as they may overlap each other. Therefore, the two classes are combined together and denoted as "Edge". The typical example of single patterns considered in this dataset is shown in Fig. 5. A total of 25 classes are determined after this pre-processing, and one thousand WBM samples are selected for each class. Among the mixed pattern types, nine of them are mixed with two single types, seven are mixed with three single types, and two mixed-type pattern are composed with four single patterns. The size of each WBM is 52×52.

We applied the detailed settings of the tensor voting and noise removal as in Wang and Chen (2022). Using a thresholding technique based on the tensor voting results, noisy points that are not a part of the patterns are eliminated. The points were removed with threshold $t = 0.32$. The parameters were set to $\alpha = 5$ and $\mu = 1$ based on experiments. The algorithms are coded using Python 3.8 and executed on a computer with a Core i9-10885H CPU@2.40 GHz. The averaged computational time similarity matching is 0.038 s per sample. The original and denoised query samples which are randomly selected for this study is illustrated in Fig. 5. Fig. 6 shows the similarity matching results of query patterns. The first nine patterns according to the rank of the similarity measure are extracted for visualization. The selected single patterns for query are arranged at the first column, and the other WBMs at the right of the black vertical line are queried patterns from the dataset. It is seen that the proposed method is able to retrieve similar patterns considering wafer rotation and pattern size for all the single patterns, when both single and mixed-type patterns exist in the historical data.

The similarity matching results with complex query patterns is shown in Fig. 7. The proposed method can identify most of the similar WBMs for the mixed-type pattern. The first row in Fig. 7 presents the query results of a mixed-type pattern that contains "Donut", "Edge", "Loc" and "Scratch". All the extracted WBMs contains at least three types of mixed patterns, showing the effectiveness in the similarity searching of mixed-type patterns. The second query pattern is composed of two defect patterns "Center" and "Loc", and most of the extracted patterns are similar except the last one. For complex patterns, the measurement of the similarity is difficult considering the combination of patterns of different shape, size and location. In this case, detecting a portion of the patterns still offers useful information for identifying root causes because the patterns are caused by numerous types of production failures that occur independently (Hsu et al., 2020).

Fig. 8 and Fig. 9 illustrate the ROC and PR curves of each query pattern, respectively. WBBS denotes the proposed weighted BBS method, and BBS represents the special case when $\alpha = 0$ and $w_v = 1$. Our method was compared with the four similarity measures, namely deformable diversity similarity (DDIS) (Talmi, Mechrez, & Zelnik-Manor, 2017), smallest deformation similarity (SDS), weighted smallest deformation

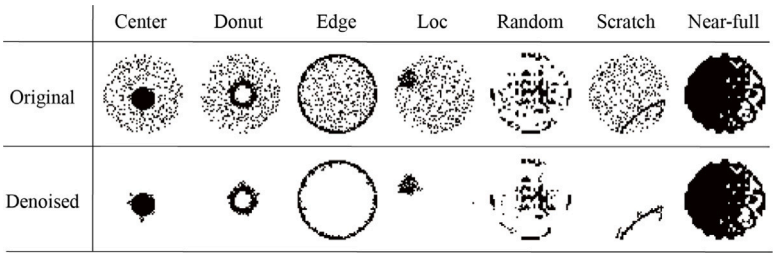

Fig. 5. Original and denoised samples of single-type query patterns.

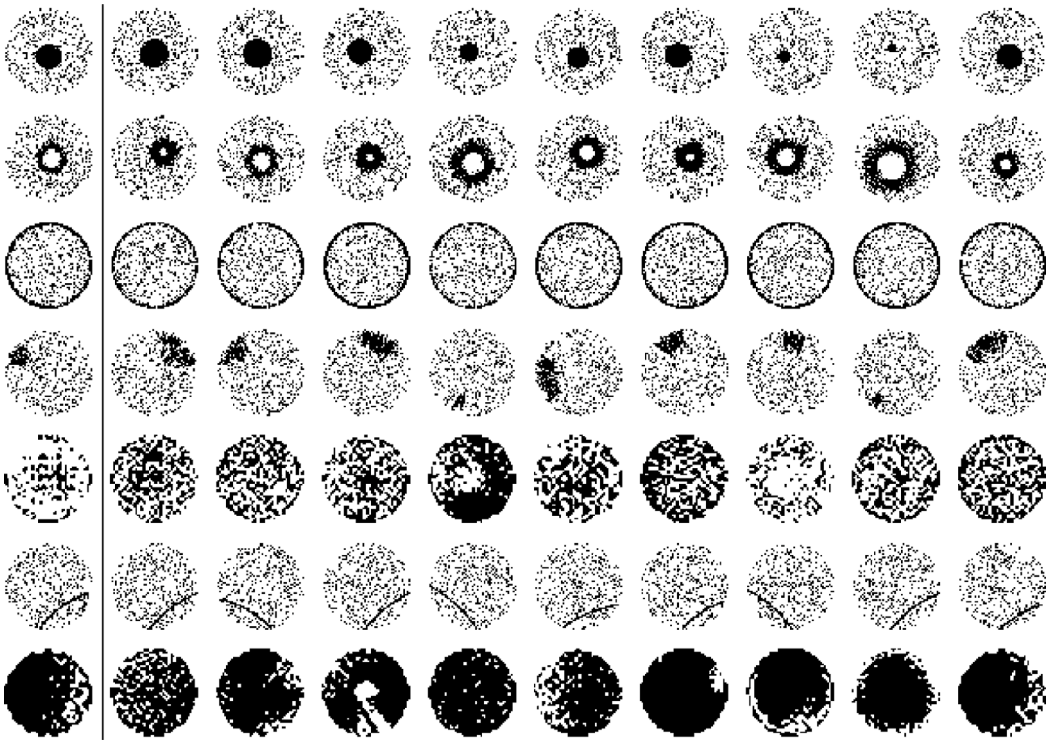

Fig. 6. Similarity matching results with single-type query patterns.

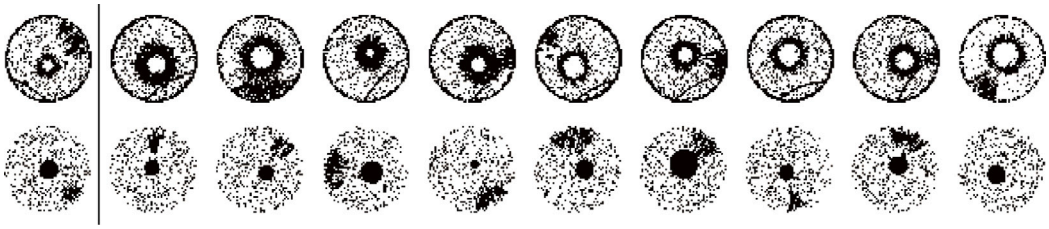

Fig. 7. Similarity matching results with mixed-type query patterns.

similarity (WSDS) (Zhang, Yang, & Gao, 2020) and Hausdorff distance (Huttenlocher, Klanderman, & Rucklidge, 1993). The results show superiority of the proposed BBS based method, particularly for WBBS, which performs the best in almost all the pattern types. Table 1 shows the corresponding average AUC and AP values for both curves. For AUC, WBBS gives the best result in all selected patterns except "Donut", where the value (0.969) is close to the best one (0.972) in BBS. For AP, WBBS shows better performance for all the selected patterns compared with other methods. The values of AP are all greater than 0.8 except for the pattern "Random", which has the AP value at 0.473. The relatively low AP is acceptable due to the fact that the "Random" pattern cannot be assigned to a specific problem during the manufacturing process, and they are probably not used for similarity searching in practice.

To evaluate the effectiveness of the tensor voting algorithm, we compared it with the mountain function (Yager & Filev, 1994) for feature transformation. WBBS was applied to both of the methods to ensure a fair comparison. In addition, comparisons were also made on whether noise removal was conducted for the WBMs. Fig. 10 shows the ROC and AP curves of similarity matching results, and the combinations of the method initials are used for illustration. "tv_d" and "tv_o" denote the application of the proposed tensor voting based method with denoised and original samples, respectively. "mt_d" and "mt_o" represent the use of the mountain function for similarity computation based on the denoised and original WBMs. In both ROC and AP results, our proposed method outperforms the mountain function, demonstrating its efficacy in extracting structural information. For both of the

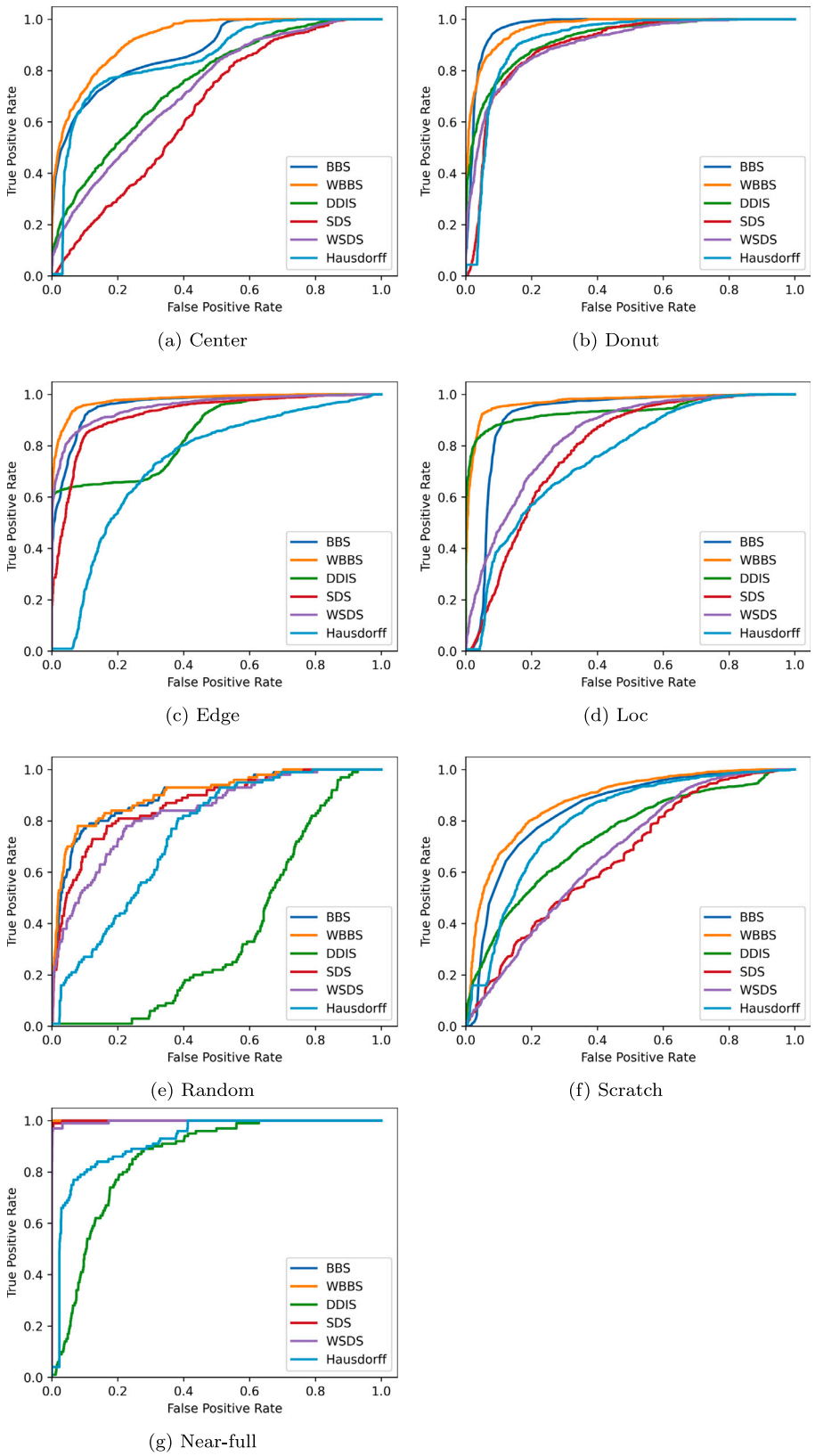

Fig. 8. Comparison of ROC curves for selected WBMs.

feature transformation methods, the denoised samples show better performance, which indicates the effectiveness of noise removal.

We then examined the influence of the weight parameter α for similarity matching. The similarity distance was calculated with different α values (0,2,5,10) and the results are shown in Fig. 11. The boxplot in Fig. 11 shows the distribution of similarity distance of the query pattern "Donut", and different colors of the box represent the number of mixed patterns included in the WBMs. For example, "3" in the

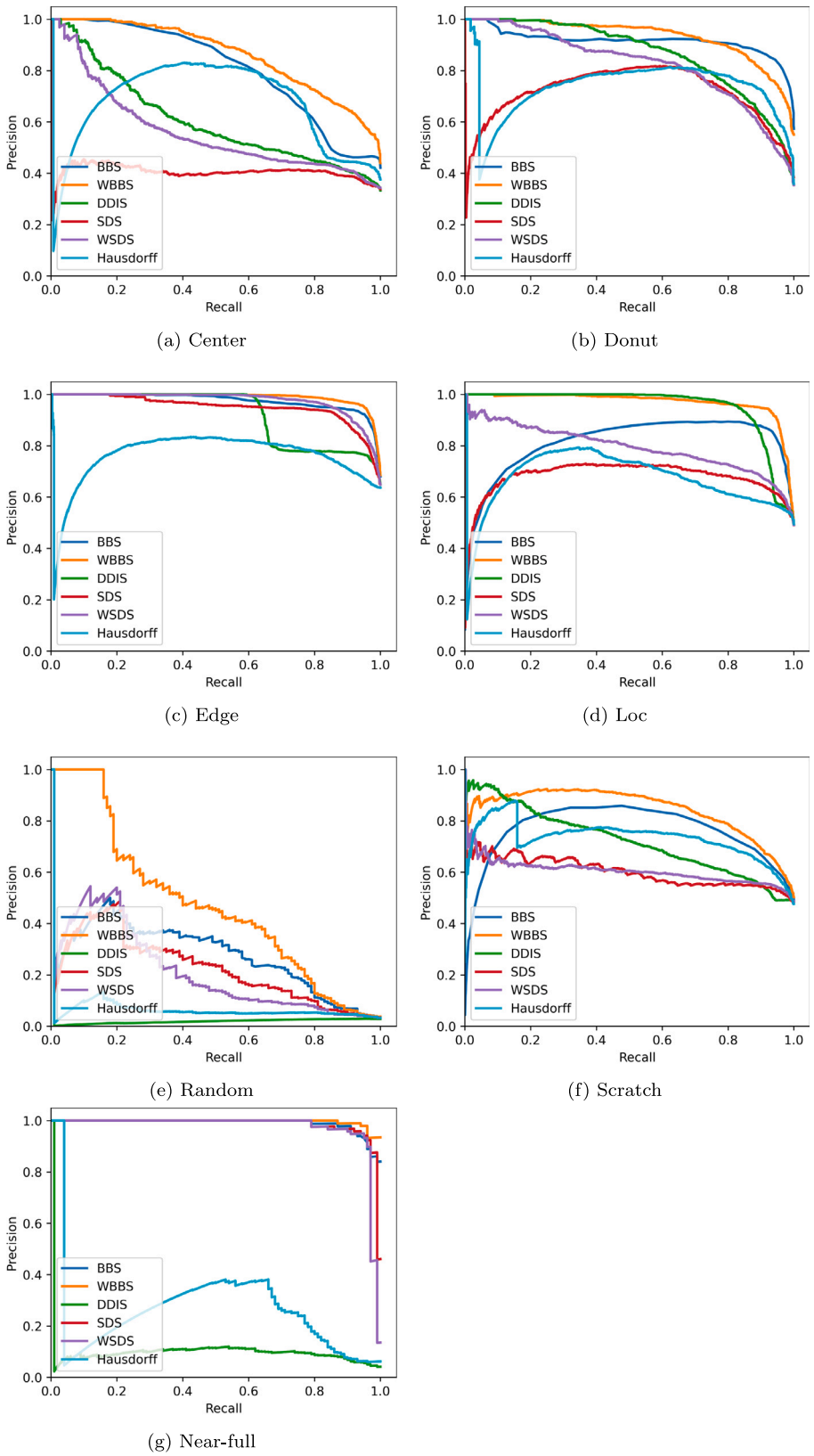

Fig. 9. Comparison of PR curves for selected WBMs.

x-axis means three patterns are contained in the same WBM, with one of them being the query pattern "Donut" shown in Fig. 6. When $\alpha = 0$, the variation in the number of defective points is not considered, and the similarity distance shows similar distribution for different number of mixed pattern types, which is consistent with our intuition. When α increases, the spread of distance distribution gradually becomes separated, indicating the effectiveness of the proposed weight. Higher values of α force the distance to be smaller if the number of defective

Table 1
Comparison of AUC and AP for selected WBMs.

Pattern type	AUC						AP					
	BBS	WBBS	DDIS	SDS	WSDS	Hausdorff	BBS	WBBS	DDIS	SDS	WSDS	Hausdorff
Center	0.876	**0.927**	0.754	0.651	0.727	0.848	0.799	**0.863**	0.605	0.407	0.560	0.671
Donut	**0.972**	0.969	0.923	0.895	0.902	0.914	0.914	**0.934**	0.868	0.711	0.824	0.739
Edge	0.960	**0.979**	0.852	0.922	0.953	0.736	0.975	**0.989**	0.920	0.950	0.975	0.761
Loc	0.915	**0.972**	0.939	0.784	0.837	0.756	0.813	**0.971**	0.953	0.676	0.794	0.669
Random	0.890	**0.910**	0.368	0.867	0.835	0.746	0.281	**0.473**	0.029	0.232	0.216	0.070
Scratch	0.843	**0.877**	0.737	0.658	0.672	0.801	0.761	**0.822**	0.721	0.601	0.604	0.731
Near-full	**1.000**	**1.000**	0.852	0.999	0.997	0.921	0.990	**0.996**	0.103	0.986	0.973	0.263
Overall	0.922	**0.948**	0.852	0.825	0.846	0.817	0.790	**0.863**	0.600	0.652	0.707	0.558

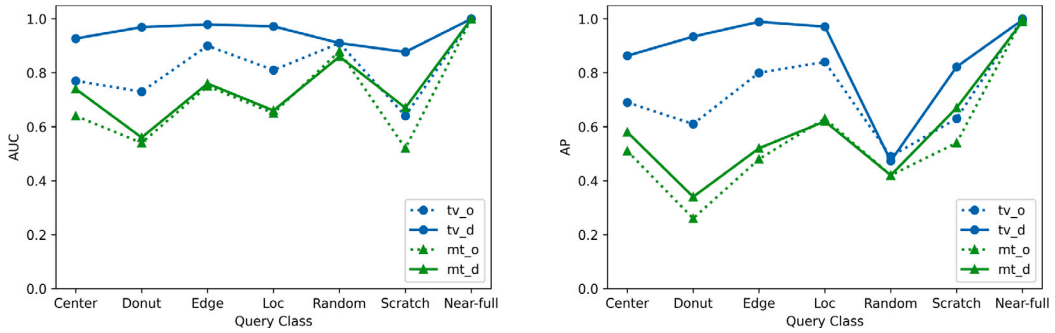

(a) AUC (b) AP

Fig. 10. Effects of feature transformation and noise removal.

points is much more than the selected pattern, which improves the query results.

The distance parameter μ has to be tuned as well, which affects the weight between the structural saliency and location information when calculating the similarity measure. In 12, it is observed that WBBS is not sensitive to μ for most of the patterns including "Center", "Donut", "Loc" and "Near-full". When $\mu = 0$, the AUC results of "Center" and "Scratch" are highly influenced, with the identification dependent on the pattern location. The similarity matching of the "Random"pattern shows significant reliance on the choice of μ, so we set μ to be 1 in this study.

4. Discussion

The proposed method can distinguish between comparable patterns when both single-type and mixed-type patterns exist in the same dataset. The method is also able to identify similar WBMs considering the effects of pattern size, density and wafer rotation. Moreover, the proposed method can be performed without any pre-defined features or classes, therefore large amount of historical training data is not required. This similarity matching method can help engineers to identify defect patterns efficiently by tracking in the history, and therefore support the diagnosis of root causes for smart productions.

In this paper, we mainly examine the problem of whether the WBM consists of a particular single pattern, due to the fact that most of the examples collected in real applications consist of only single pattern types. Matching with a single pattern is also easier to consider and produces more accurate results. In addition, a mixed-type pattern can be identified by combining the thresholding results of the related single patterns and the similarity distance with the chosen single pattern, which provides useful information for pattern identification. In this situation, various patterns can be utilized as matching templates to derive similarity indices, which can then be employed as features for the WBM classification task.

For WBM similarity searching, the parameters need to be determined are α and μ. α controls the degree of similarity difference for patterns with different numbers of defective dies. Greater values of α penalizes this variation, which gives smaller similarity measure when the density of defects in WBMs are significantly different. μ controls the weight of the strength between the structural saliency and the location information. Greater values of μ emphasize the importance of pattern location for the determination of the WBM similarity. The weight parameters α and distance parameter μ used for similarity calculation can be separated chosen for different patterns, as the effects of these parameters on different patterns may be significantly different.

Furthermore, we define w_p as the minimum number of defective points in the two sets to be compared because of the range of the similarity distance and the commutative property for computation. It should be noted that w_p can be flexibly defined in different forms based on real-world settings, resulting in different similarity ranking results for mixed-type patterns. As an example, $w_p = \frac{1}{N}$ makes the similarity measure of different samples comparable considering a query pattern, where N is the number of defective points on the query pattern. Then for a selected pattern, the extracted similar patterns will tend to be of mixed-type that consist of at least the query pattern in the WBM, because the BBS distances remain the same for different numbers of mixed pattern types. Similarly, w_v can be designed to account for the number difference of defective points.

5. Conclusion

In this paper, we propose a novel similarity searching method for WBMs with mixed-type patterns. Using tensor voting, the structural information of the defect patterns is first highlighted. The WBBS method is then proposed to support expert judgments, to find the root causes of the patterns, based on the structural saliency and location information of the defect patterns. The similarity measure are designed to give similar scores with the same pattern contained, while considering the exact similarity when the number of defective points are really different. Experiments show the superiority of the proposed method in the identification of defect patterns when both single and mixed-type patterns are present.

For future studies, the parameters used for similarity calculation can be separated chosen for different patterns. Furthermore, the structural

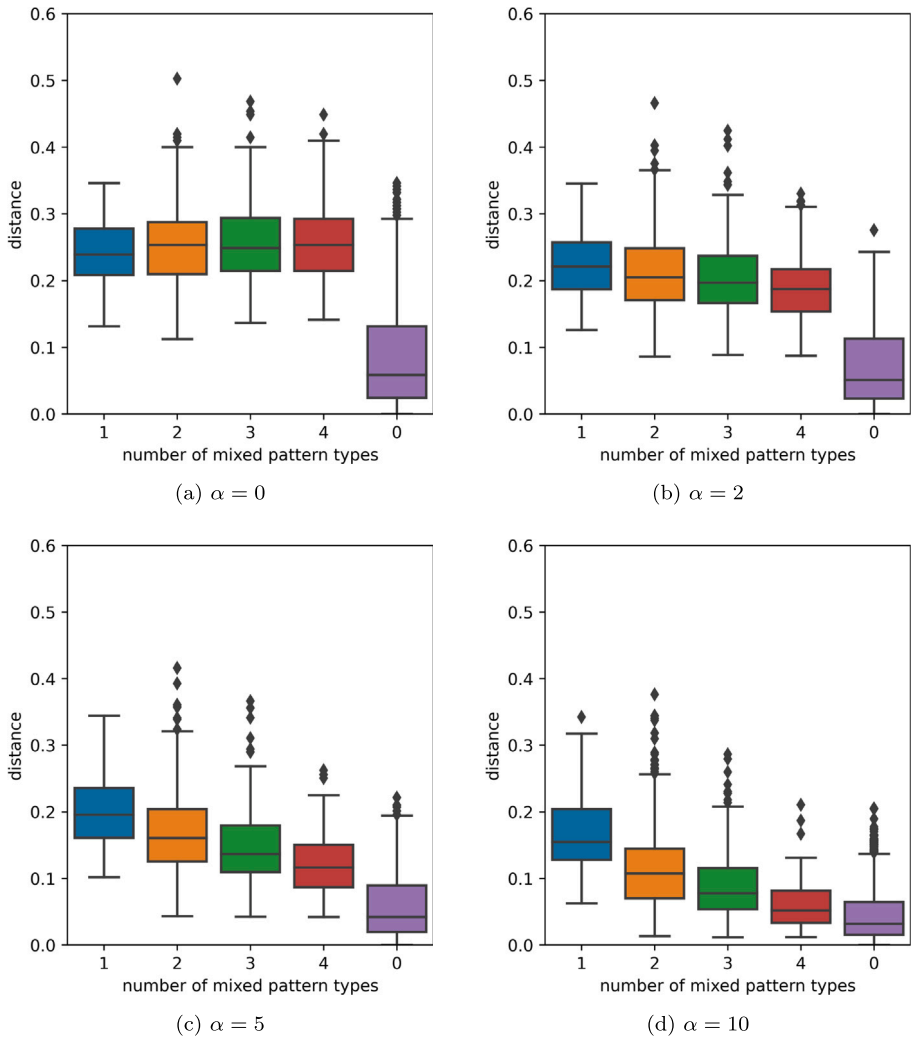

Fig. 11. The influence of different α for weight calculation in similarity measure.

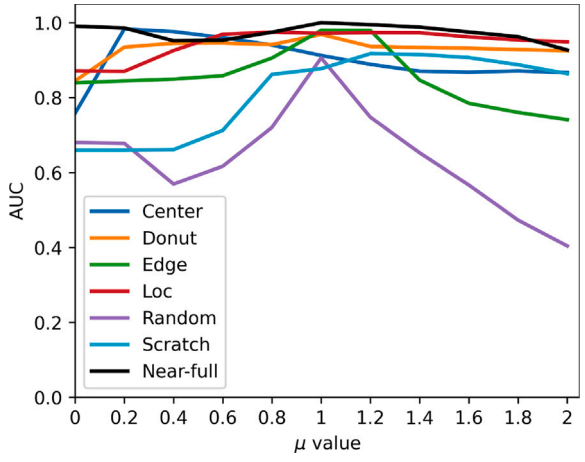

Fig. 12. Effects of the choice of μ on similarity searching results.

data produced through tensor voting offers the opportunity for the identification and extraction of single patterns in mixed-type scenarios. This method can be used to resolve other comparable problems, to support the decision making in tasks of fault diagnosis in intelligent manufacturing systems.

CRediT authorship contribution statement

Rui Wang: Conceptualization, Methodology, Software, Formal analysis, Data curation, Writing – original draft, Supervision, Funding acquisition. **Songhao Wang:** Methodology, Validation, Investigation, Resources, Writing – review & editing, Visualization, Project administration, Funding acquisition.

Data availability

We use public data in this research, which can be found in the reference.

References

Adly, F., Alhussein, O., Yoo, P. D., Al-Hammadi, Y., Taha, K., Muhaidat, S., et al. (2015). Simplified subspaced regression network for identification of defect patterns in semiconductor wafer maps. *IEEE Transactions on Industrial Informatics*, *11*(6), 1267–1276.

Dou, R., He, Z., & Hsu, C.-Y. (2018). Foreword: Smart manufacturing, innovative product and service design to empower Industry 4.0. *Computer & Industrial Engineering*, *125*, 514–516.

Du, J., Yan, H., Chang, T.-S., & Shi, J. (2022). A tensor voting-based surface anomaly classification approach by using 3D point cloud data. *Journal of Manufacturing Science and Engineering*, *144*(5), Article 051005.

Hsu, C.-Y., Chen, W.-J., & Chien, J.-C. (2020). Similarity matching of wafer bin maps for manufacturing intelligence to empower Industry 3.5 for semiconductor manufacturing. *Computers & Industrial Engineering*, *142*, Article 106358.

Hsu, S.-C., & Chien, C.-F. (2007). Hybrid data mining approach for pattern extraction from wafer bin map to improve yield in semiconductor manufacturing. *International Journal of Production Economics*, *107*(1), 88–103.

Hsu, C.-Y., & Chien, J.-C. (2022). Ensemble convolutional neural networks with weighted majority for wafer bin map pattern classification. *Journal of Intelligent Manufacturing*, *33*(3), 831–844.

Huang, D.-L., Du, S.-C., Li, G.-L., & Wu, Z.-Q. (2017). A systematic approach for online minimizing volume difference of multiple chambers in machining processes based on high-definition metrology. *ASME Transactions on Manufacturing Science and Engineering*, *139*(8), Article 081003.

Huttenlocher, D. P., Klanderman, G. A., & Rucklidge, W. J. (1993). Comparing images using the Hausdorff distance. *IEEE Transactions on Pattern Analysis and Machine Intelligence*, *15*(9), 850–863.

Hwang, J., & Kim, H. (2020). Variational deep clustering of wafer map patterns. *IEEE Transactions on Semiconductor Manufacturing*, *33*(3), 466–475.

Kang, H., & Kang, S. (2021). A stacking ensemble classifier with handcrafted and convolutional features for wafer map pattern classification. *Computers in Industry*, *129*, Article 103450.

Kim, J., Lee, Y., & Kim, H. (2018). Detection and clustering of mixed-type defect patterns in wafer bin maps. *IISE Transactions*, *50*(2), 99–111.

Kyeong, K., & Kim, H. (2018). Classification of mixed-type defect patterns in wafer bin maps using convolutional neural networks. *IEEE Transactions on Semiconductor Manufacturing*, *31*(3), 395–402.

Lee, J. H., Moon, I.-C., & Oh, R. (2021). Similarity search on wafer bin map through nonparametric and hierarchical clustering. *IEEE Transactions on Semiconductor Manufacturing*, *34*(4), 464–474.

Lee, J. H., Yu, S. J., & Park, S. C. (2001). Design of intelligent data sampling methodology based on data mining. *IEEE Transactions on Robotics and Automation*, *17*(5), 637–649.

Li, G., Du, S., Huang, D., Zhao, C., & Deng, Y. (2019). Dynamics modeling-based optimization of process parameters in face milling of workpieces with discontinuous surfaces. *ASME Transactions on Manufacturing Science and Engineering*, *141*(10), Article 101009.

Li, G., Du, S., Wang, B., Lv, J., & Deng, Y. (2022). High definition metrology-based quality improvement of surface texture in face milling of workpieces with discontinuous surfaces. *ASME Transactions on Manufacturing Science and Engineering*, *144*(3), Article 031001.

Liao, C.-S., Hsieh, T.-J., Huang, Y.-S., & Chien, C.-F. (2013). Similarity searching for defective wafer bin maps in semiconductor manufacturing. *IEEE Transactions on Automation Science and Engineering*, *11*(3), 953–960.

Liao, C.-S., Hsieh, T.-J., Huang, Y.-S., & Chien, C.-F. (2014). Similarity searching for defective wafer bin maps in semiconductor manufacturing. *IEEE Transactions on Automation Science and Engineering*, *11*(3), 953–960.

Medioni, G., Tang, C.-K., & Lee, M.-S. (2000). Tensor voting: Theory and applications. In *Proceedings of RFIA, vol. 2000*.

Mordohai, P., & Medioni, G. (2010). Dimensionality estimation, manifold learning and function approximation using tensor voting.. *Journal of Machine Learning Research*, *11*(1).

Nakazawa, T., & Kulkarni, D. V. (2018). Wafer map defect pattern classification and image retrieval using convolutional neural network. *IEEE Transactions on Semiconductor Manufacturing*, *31*(2), 309–314.

Oron, S., Dekel, T., Xue, T., Freeman, W. T., & Avidan, S. (2017). Best-buddies similarity—Robust template matching using mutual nearest neighbors. *IEEE Transactions on Pattern Analysis and Machine Intelligence*, *40*(8), 1799–1813.

Piao, M., Jin, C. H., Lee, J. Y., & Byun, J.-Y. (2018). Decision tree ensemble-based wafer map failure pattern recognition based on radon transform-based features. *IEEE Transactions on Semiconductor Manufacturing*, *31*(2), 250–257.

Qin, Y., Zhang, J., Chan, F. T., Chung, S., Niu, B., & Qu, T. (2020). A two-stage optimization approach for aircraft hangar maintenance planning and staff assignment problems under MRO outsourcing mode. *Computers & Industrial Engineering*, *146*, Article 106607.

Saito, T., & Rehmsmeier, M. (2015). The precision-recall plot is more informative than the ROC plot when evaluating binary classifiers on imbalanced datasets. *PLoS One*.

Shin, W., Kahng, H., & Kim, S. B. (2022). Mixup-based classification of mixed-type defect patterns wafer bin maps. *Computers & Industrial Engineering*, *167*, Article 107996.

Talmi, I., Mechrez, R., & Zelnik-Manor, L. (2017). Template matching with deformable diversity similarity. In *Proceedings of the IEEE conference on computer vision and pattern recognition* (pp. 175–183).

Wang, R., & Chen, N. (2022). Detection and recognition of mixed-type defect patterns in wafer bin maps via tensor voting. *IEEE Transactions on Semiconductor Manufacturing*, *35*(3), 485–494.

Wang, R., & Wang, S. (2022). Tensor voting based similarity matching of wafer bin maps in semiconductor manufacturing. In *2022 5th international conference on data science and information technology* (pp. 1–6). IEEE.

Wang, J., Xu, C., Yang, Z., Zhang, J., & Li, X. (2020). Deformable convolutional networks for efficient mixed-type wafer defect pattern recognition. *IEEE Transactions on Semiconductor Manufacturing*, *33*(4), 587–596.

Wu, M.-J., Jang, J.-S. R., & Chen, J.-L. (2014). Wafer map failure pattern recognition and similarity ranking for large-scale data sets. *IEEE Transactions on Semiconductor Manufacturing*, *28*(1), 1–12.

Wu, T.-P., Yeung, S.-K., Jia, J., Tang, C.-K., & Medioni, G. (2011). A closed-form solution to tensor voting: Theory and applications. *IEEE Transactions on Pattern Analysis and Machine Intelligence*, *34*(8), 1482–1495.

Yager, R., & Filev, D. (1994). Approximate clustering via the mountain method. *IEEE Transactions on Systems, Man, and Cybernetics*, *24*(8), 1279–1284.

Yu, J., & Lu, X. (2015). Wafer map defect detection and recognition using joint local and nonlocal linear discriminant analysis. *IEEE Transactions on Semiconductor Manufacturing*, *29*(1), 33–43.

Yuan, T., & Kuo, W. (2008). Spatial defect pattern recognition on semiconductor wafers using model-based clustering and Bayesian inference. *European Journal of Operational Research*, *190*(1), 228–240.

Zhang, C., Yan, H., Lee, S., & Shi, J. (2018a). Multiple profiles sensor-based monitoring and anomaly detection. *Journal of Quality Technology*, *50*(4), 344–362.

Zhang, C., Yan, H., Lee, S., & Shi, J. (2018b). Weakly correlated profile monitoring based on sparse multi-channel functional principal component analysis. *IISE Transactions*, *50*(10), 878–891.

Zhang, Z., Yang, X., & Gao, H. (2020). Weighted smallest deformation similarity for NN-based template matching. *IEEE Transactions on Industrial Informatics*, *16*(11), 6787–6795.

Zhu, J., Huang, C.-G., Shen, C., & Shen, Y. (2022). Cross-domain open-set machinery fault diagnosis based on adversarial network with multiple auxiliary classifiers. *IEEE Transactions on Industrial Informatics*, *18*(11), 8077–8086.